

Development of diethylcarbamazine-loaded poly(caprolactone) nanoparticles for anti-inflammatory purpose: Preparation and characterization

Henrique Rodrigues Marcelino^{1,a}, Brennda Martins Gabinio^{2,a},
Marine Nascimento de Lima², Silvana Cartaxo da Costa Urtiga²,
Gabriel Barros Rodrigues³, Bruna Braga Dantas⁴,
Demétrius Antônio Machado de Araújo⁴,
Christina Alves Peixoto⁴, Elquio Eleamen Oliveira^{2*}

^aThe authors share the first authorship of the manuscript. ¹Faculty of Pharmacy, Federal University of Bahia, Salvador/BA, Brazil, ²Laboratory of Synthesis and Vectorization of Molecules (LSVM), State University of Paraíba, João Pessoa/PB, Brazil, ³Laboratory of Ultrastructure, Institute Aggeu Magalhães, FIOCRUZ, Recife/PE, Brazil, ⁴Biotechnology Center, Federal University of Paraíba, João Pessoa/PB, Brazil

Diethylcarbamazine-loaded nanoparticles were previously evaluated for their anti-inflammatory activity. However, little is known regarding their physicochemical properties. Thus, the purpose of this study was to physicochemically characterize diethylcarbamazine-loaded poly(caprolactone) nanoparticles and evaluate their *in vitro* cytotoxicity. All formulations were prepared using the double-emulsion method. The average particle size was in the ranged between 298 and 364 nm and the polydispersity indexes were below 0.3. The zeta potential values were marginally negative, which may be related to drug loading, as higher loading led to an increase in the modulus of the zeta potential values. Fourier transform infrared spectroscopy (FT-IR) and X-ray powder diffraction (XRD) analysis did not reveal any chemical interactions between the chemicals used and the absence of drug in crystalline form on the nanoparticle surfaces. The *in vitro* drug release study revealed a concentration-dependent release from the nanoparticles into the medium. The *in vitro* cytotoxicity assay demonstrated the biocompatibility of the blank and loaded nanoparticles. Hence, all formulations presented good physicochemical and safety properties, corroborating the *in vivo* anti-inflammatory activity, previously reported by our group.

Keywords: Diethylcarbamazine. Polymeric nanoparticles. Physicochemical properties. *In vitro* biocompatibility.

INTRODUCTION

Diethylcarbamazine (DEC) is one of the main drugs used in the treatment of lymphatic filariasis and has excellent tolerability with few side effects (Ali *et al.*, 2014; Peixoto, Silva, 2014). This drug is widely

commercialized as a citrate salt, presenting high water solubility and good stability, although it has a short half-life. In addition to its anti-filariasis effects, the anti-inflammatory effects of DEC have been reported based on the metabolism of arachidonic acid and the inhibition of cyclooxygenase, lipoxigenase, and nuclear factor kappa-B (NF- κ B) pathways in humans (Peixoto, Silva, 2014). Thus, the anti-inflammatory potential of DEC has been evaluated in acute and chronic hepatic inflammatory models, with potential pre-clinical responses observed (Rodrigues *et al.*, 2017; Rocha *et al.*, 2012; Silva *et al.*, 2014).

*Correspondence: E. E. Oliveira. Laboratório de Síntese e Vetorização de Moléculas. Centro de Ciências Biológicas e Sociais Aplicadas. Universidade Estadual da Paraíba. Rua Horácio Trajano, S/N, Cristo Redentor. João Pessoa/PB, 58070-450, Brazil. Phone +55 83 3223-6702. E-mail: elquioeleamen@yahoo.com.br
ORCID: <https://orcid.org/0000-0002-7214-4455>
Brennda Martins Gabinio ORCID: <https://orcid.org/0000-0002-8590-5962>

Recently, our research group has revealed the effectiveness of DEC-loaded nanoparticles (BR 10 2017 002700-7 and PCT/BR2018/050027) in an induced murine model of inflammation. Interestingly, the nanoparticles have demonstrated the ability to enhance the therapeutic activity of DEC using a dose of 12.5 mg/kg for 6 days, which is less than that reported previously (50 mg/kg) (Rocha *et al.*, 2012; Silva *et al.*, 2014). The enhanced activity may have been a consequence of the improved residence time of the drug-loaded nanoparticles (Rodrigues *et al.*, 2017; Rodrigues *et al.*, 2018).

As described in our previous works, the simple nanoencapsulation of DEC, which has led to an enhanced pharmacological activity, is dependent on several pre-formulation studies. In general, pre-clinical studies rely on a good characterization of the formulation (Aguirre *et al.*, 2016). The interactions of drug-excipients and excipients, as well as the ability of the nanoparticles to control drug release, are the most common concerns before biological efficacy evaluation (Fathima *et al.*, 2011; Gressl *et al.*, 2017). In addition, the biopharmaceutical studies of nanocarriers usually involve the characterization of their toxicities against different cell lines, as a pre-evaluation of the nanoparticle toxicity (Costa *et al.*, 2014).

Hence, the goal of this study was to present the experiments performed to develop DEC-loaded nanoparticles with reported anti-inflammatory activity (Rodrigues *et al.*, 2017; Rodrigues *et al.*, 2018). Herein, physical, chemical, and biological characterizations were performed to obtain a nanocarrier that could be able to be pre-clinically evaluated in terms of its anti-inflammatory activity.

MATERIAL AND METHODS

Initially, 1 mL of an aqueous solution containing 10 (NP_DEC10) or 25 mg (NP_DEC25) of DEC (Sigma Aldrich®, São Paulo, Brazil) was emulsified in 10 mL of dichloromethane containing 50 mg of polycaprolactone (PCL) and 30 mg of Pluronic® F68. The first emulsification was performed using a homogenizer (Ultra-Turrax® T18, IKA, Germany) at 25,000 rpm to obtain a water/oil emulsion. The second emulsification was achieved by adding a second aqueous phase solution containing

0.5%_(w/v) polyvinyl alcohol (PVA, molecular weight (MW) = 13,000 – 23,000 Da) to its composition. The second emulsification was performed using an Ultra-Turrax® T18 at 25,000 rpm. Both emulsification steps were carried out for 10 min in an ice bath. The solvent was evaporated under reduced pressure (RV-10 basic, IKA, Germany). The final dispersion was frozen at -80°C and freeze-dried (Alpha 1-2 LDplus, Christ, France) using a 24-hour cycle. Blank nanoparticles (NP_blank) were prepared using the same protocol without the addition of DEC.

The average particle size and polydispersity index were measured using the ZetaSizer Nano ZS instrument (Malvern Instruments, United Kingdom). The nanoparticle dispersion was diluted (1:99 ratio) in ultrapure water. Subsequently, the same dilution was used to measure the zeta potential, also using the ZetaSizer Nano ZS instrument (Malvern Instruments, United Kingdom). Both measurements were performed in triplicate at 25°C.

Nanoparticle morphology was examined using a transmission electron microscopy (TEM) apparatus (Tecnai G20, FEI, United States). For sample preparation, a drop of the nanoparticle suspension was placed on a carbon-coated copper grid and then negatively stained with a 2% phosphotungstic acid solution. The grid was dried at room temperature and observed using TEM.

Attenuated total reflection–Fourier transform infrared (ATR-FTIR) spectroscopy measurements were performed in the solid-state using a spectrophotometer (Shimadzu® IRPrestige-21, United States). The samples were placed onto a small crystal area, and the pressure arm was positioned over the sample. All spectra were obtained after 20 scans in the range of 4000 cm⁻¹ to 700 cm⁻¹ at room temperature.

X-Ray diffraction (XRD) measurements were performed using the diffractometer (model D8 Advance, Bruker, United Kingdom) with a copper anode (Cu K α radiation, $\lambda = 0,15418$ nm, 40 kV, 20 mA). Along with the nanoparticle samples, all raw materials were analyzed at a scanning rate of 2°/min, in the range of 5-50°.

The encapsulation efficiency (EE) of DEC in the formulations was determined by extraction of DEC from the nanoparticles with an excess of water using a dialysis bag until complete extraction (5 days). The

extracted drug was quantified by UV spectrophotometry (SP2000UV, Spectrum, Brazil) at $\lambda = 211$ nm ($y = 0.0228x + 0.0088$, $R^2 = 0.999$). The following equation was used to express the results: %EE = (extracted drug/total drug added) \times 100.

Drug release studies were performed for both formulations (NP_DEC10 and NP_DEC25), and water was used as the dissolution medium. Briefly, the nanoparticles were placed in dialysis bags (MW cut-off 12,000 Da, Sigma-Aldrich®, Brazil), sealed and dropped into 100 mL of medium. The system was maintained at $37^\circ \pm 2^\circ\text{C}$ with continuous magnetic stirring at 100 rpm. Aliquots (2 mL) were withdrawn at predetermined time points and immediately replaced with the same volume of the dissolution medium. The quantification of DEC was determined by UV spectrophotometry (SP2000UV, Spectrum, Brazil) at 211 nm.

To determine the mechanism of drug release from the formulations, the experimental data were fitted to different kinetic models using Excel® add-in DDSolver (Zhang *et al.*, 2010). The main mathematical models were analyzed (Table I). The model that best described

the release data was evaluated based on the adjusted coefficient of determination (adjusted-R²), the standard deviation of the residuals (RMSE) and model selection criterion (MSC).

The nanoparticle cytotoxicity was evaluated using the colorimetric MTT (3-(4,5-dimethylthiazol-2-yl)-2,5-diphenyltetrazolium bromide) assay (7). Human umbilical vein endothelial cells (HUVECs) were plated in 96 well plates at a density of 3×10^4 cells/mL and incubated for 24 h and 72 h, at 37°C , in a humidified atmosphere containing 5% of CO₂. Subsequently, MTT (5mg/mL in phosphate buffer solution) was incubated for 3 h under the same conditions as described above. The MTT formazan product was dissolved in sodium dodecyl sulfate (SDS)/HCl 0.01 mol/L and the optical density was recorded in a plate reader at 570 nm. DEC concentrations ranging between 6 and 200 $\mu\text{g/mL}$ were used for NP_DEC10 and NP_DEC25, for the blank formulation, the corresponding volume of NP_DEC10 was used. Furthermore, to evaluate the difference among group populations, ANOVA was performed, followed by the Bonferroni post hoc test.

TABLE I - Evaluation of different kinetic models for the drug release of DEC from the nanoparticles prepared

Sample	Model	Equation	R2 Adjusted	RMSE	Constants	MSC
NP_DEC10 (3 hours)	Zero-order	$F = k_0 \times t$	0.92	6.49	$K0 = 25.29$	2.47
	First-order	$F = F_{\max} \times [1 - \text{Exp}(-k_1 \times t)]$	0.95	4.69	$K1 = 0.36$	3.36
	Higuchi	$F = k_H \times t^{0.5}$	0.89	7.79	$kH = 35.44$	2.03
	Korsmeyer-Peppas	$F = k_{kp} \times t^n$	0.95	4.40	$kKP = 30.73$	3.52
	Peppas-Sahlin	$F = k_1 \times t^m + k_2 \times t^{(2 \times m)}$	0.95	4.47	$k1 = -18.32; k2 = 49.87; m = 0.29$	3.58
NP_DEC25 (3 hours)	Zero-order	$F = k_0 \times t$	0.92	6.49	$k0 = 25.29$	2.47
	First-order	$F = F_{\max} \times [1 - \text{Exp}(-k_1 \times t)]$	0.95	4.69	$k1 = 0.36$	3.36
	Higuchi	$F = k_H \times t^{0.5}$	0.89	7.79	$kH = 35.44$	2.03
	Korsmeyer-Peppas	$F = k_{kp} \times t^n$	0.95	4.40	$kKP = 30.73$	3.52
	Peppas-Sahlin	$F = k_1 \times t^m + k_2 \times t^{(2 \times m)}$	0.95	4.47	$k1 = -18.32; k2 = 49.87; m = 0.29$	3.58

(continues on the next page...)

TABLE 1 - Evaluation of different kinetic models for the drug release of DEC from the nanoparticles prepared

Sample	Model	Equation	R2 Adjusted	RMSE	Constants	MSC
NP_ DEC10 (24 hours)	Zero-order	$F = k_0 \times t$	-0.02	28.10	$k_0 = 0.09$	-0.10
	First-order	$F = F_{\max} \times [1 - \text{Exp}(-k_1 \times t)]$	0.96	4.45	$k_1 = 0.005$	3.74
	Higuchi	$F = k_H \times t^{0.5}$	0.83	11.51	$k_H = 3.07$	1.68
	Korsmeyer-Peppas	$F = k_{KP} \times t^n$	0.87	10.21	$k_{KP} = 5.31$	1.86
	Peppas-Sahlin	$F = k_1 \times t^m + k_2 \times t^{(2 \times m)}$	0.98	3.69	$k_1 = 1.30; k_2 = -0.01; m = 0.81$	4.01
NP_ DEC25 (24 hours)	Zero-order	$F = k_0 \times t$	-0.46	39.12	$k_0 = 0.10$	-0.52
	First-order	$F = F_{\max} \times [1 - \text{Exp}(-k_1 \times t)]$	0.98	4.20	$k_1 = 0.01$	4.12
	Higuchi	$F = k_H \times t^{0.5}$	0.69	17.91	$k_H = 3.69$	1.04
	Korsmeyer-Peppas	$F = k_{KP} \times t^n$	0.81	14.29	$k_{KP} = 9.12$	1.43
	Peppas-Sahlin	$F = k_1 \times t^m + k_2 \times t^{(2 \times m)}$	0.97	5.19	$k_1 = 1.84, k_2 = -0.01; m = 0.72$	3.46

RESULTS AND DISCUSSION

The DEC-loaded nanoparticles herein studied have been previously evaluated for their pharmacological effectiveness (Rodrigues *et al.*, 2017; Rodrigues *et al.*, 2018). In the present study, we revealed the physicochemical properties that enabling their success as an alternative for the treatment of inflammatory diseases.

The TEM images (Figure 1A) indicated that all formulations demonstrated a spherical shape and an absence of aggregates. A spherical shape is usually

observed in nanoparticles based on caprolactone polymers prepared by the double-emulsification method (Barba *et al.*, 2014; Iqbal *et al.*, 2015). Additionally, the average particle sizes observed were 284 ± 2 nm, 300 ± 4 nm, and 329 ± 2 nm, for NP_blank, NP_DEC10, and NP_DEC25, respectively. Furthermore, the measured zeta potential values were -3.4 ± 0.4 mV, -3.7 ± 0.21 mV, and -8.17 ± 0.8 mV, and the assessed polydispersity indexes were 0.14 ± 0.03 , 0.17 ± 0.02 , and 0.26 ± 0.011 , for the NP_blank, NP_DEC10, and NP_DEC25, respectively.

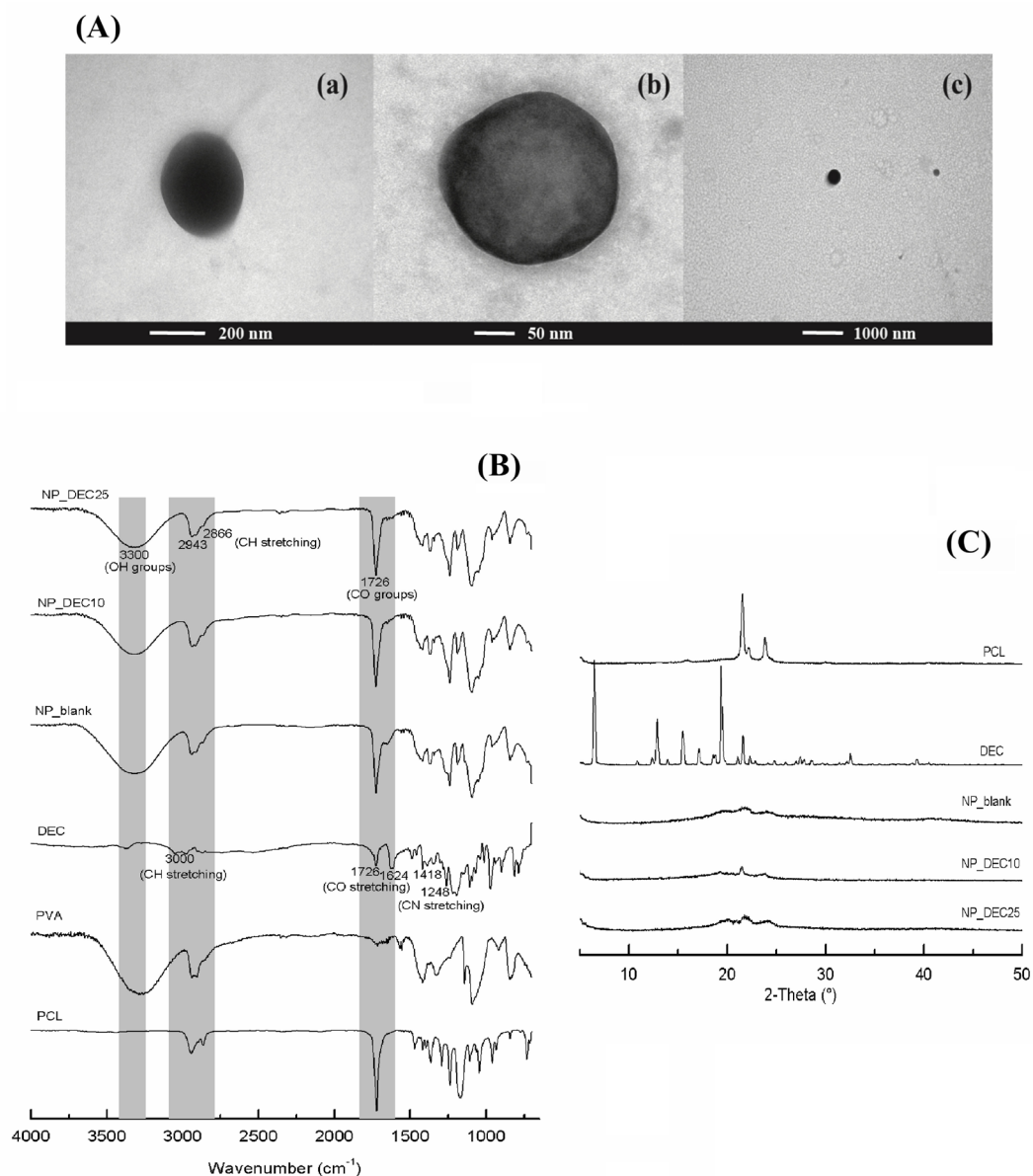


FIGURE 1 - (A) TEM of (a) NP_blank, (b) NP_DEC10, and (c) NP_DEC25. (B) ATR FT-IR spectra of the raw materials and nanoparticles produced. (C) XRD of the raw materials and nanoparticles produced. TEM, transmission electron microscopy; ATR FT-IR, attenuated total reflection–Fourier transform infrared; XRD, X-ray powder diffraction.

All formulations demonstrated monomodal particle size distributions; however, statistical differences could be observed in the polydispersity index values. DEC-loaded nanoparticles indicated statistical differences between both formulations and when compared with the blank formulation. This difference may be related to the entrapment of DEC since it resulted in altered zeta potential values. We hypothesize that the adsorption of DEC molecules onto the surface of the nanoparticles leads

to a higher negative charge. This hypothesis corroborated with the XRD and the *in vitro* drug release findings discussed later.

The FT-IR spectra of DEC, PCL, NP_blank, NP_DEC10, and NP_DEC25 are shown in Figure 1B. The FT-IR spectrum of DEC demonstrated all the characteristic peaks of the drug, with bands at 3000, 1726 and 1624, 1418 and 1248 cm^{-1} due to CH stretching, CO stretching, and CN stretching, respectively (Chaves *et al.*, 2013). The FT-IR

spectrum of PCL exhibited characteristic peaks at 2943 and 2866 cm^{-1} (CH stretching) and 1726 cm^{-1} (CO stretching). Additionally, a new peak appeared at close to 3000 cm^{-1} , which can be related to the OH groups present in PVA used as a stabilizing agent in the nanoparticle formulations. Thus, all nanoparticles presented markedly similar spectra to those of PCL and PVA, and the peaks were related to the DEC overlap due to encapsulation, which is expected as the amount of polymer used was higher than that of the drug.

XRD patterns of DEC, PCL, blank nanoparticles, and formulations of DEC-loaded nanoparticles are shown in Figure 1C. The diffractogram of the DEC indicated that the drug was in the crystalline form. The XRD of PCL demonstrated two major peaks at 21.5° and 23.8° at 2 θ , confirming its semi-crystalline structure (Ciardelli *et al.*, 2005). The XRD patterns of the blank and DEC-loaded nanoparticles were amorphous. Thus, it can be suggested that the DEC is homogeneously dispersed in the polymeric matrix. Notably, all the nanoparticles lost the characteristic peak of the raw material PCL, which reveals the impact of the production method used over the final form of the raw materials (Mensink *et al.*, 2017).

NP_DEC10 and NP_DEC25 demonstrated an EE of $64.51 \pm 4.41\%$ and $70.97 \pm 1.41\%$, respectively. Compared with other hydrophilic molecules, these values can be considered high when encapsulated in PCL nanoparticles. In this study, the high EE can be attributed to the production method used. The double-emulsification method (w/o/w) presented an internal water vesicle that facilitated the entrapment of hydrophilic drugs in the hydrophobic matrices (Araujo *et al.*, 2013).

The drug release profile for both formulations was characterized by an initial rapid release, followed by a sustained drug release phase (Figure 2). After 3 h, approximately 50% and 73% of DEC was released from NP_DEC10 and NP_DEC25, respectively. An initial rapid release is known as a burst effect and could correspond to DEC molecules adsorbed onto the surface of nanoparticles and readily available for released from the polymeric matrix. From a clinical standpoint, burst release might be a tool to approach the therapeutic window of a drug, and sustained release will maintain a constant concentration, also known as steady state, for longer periods.

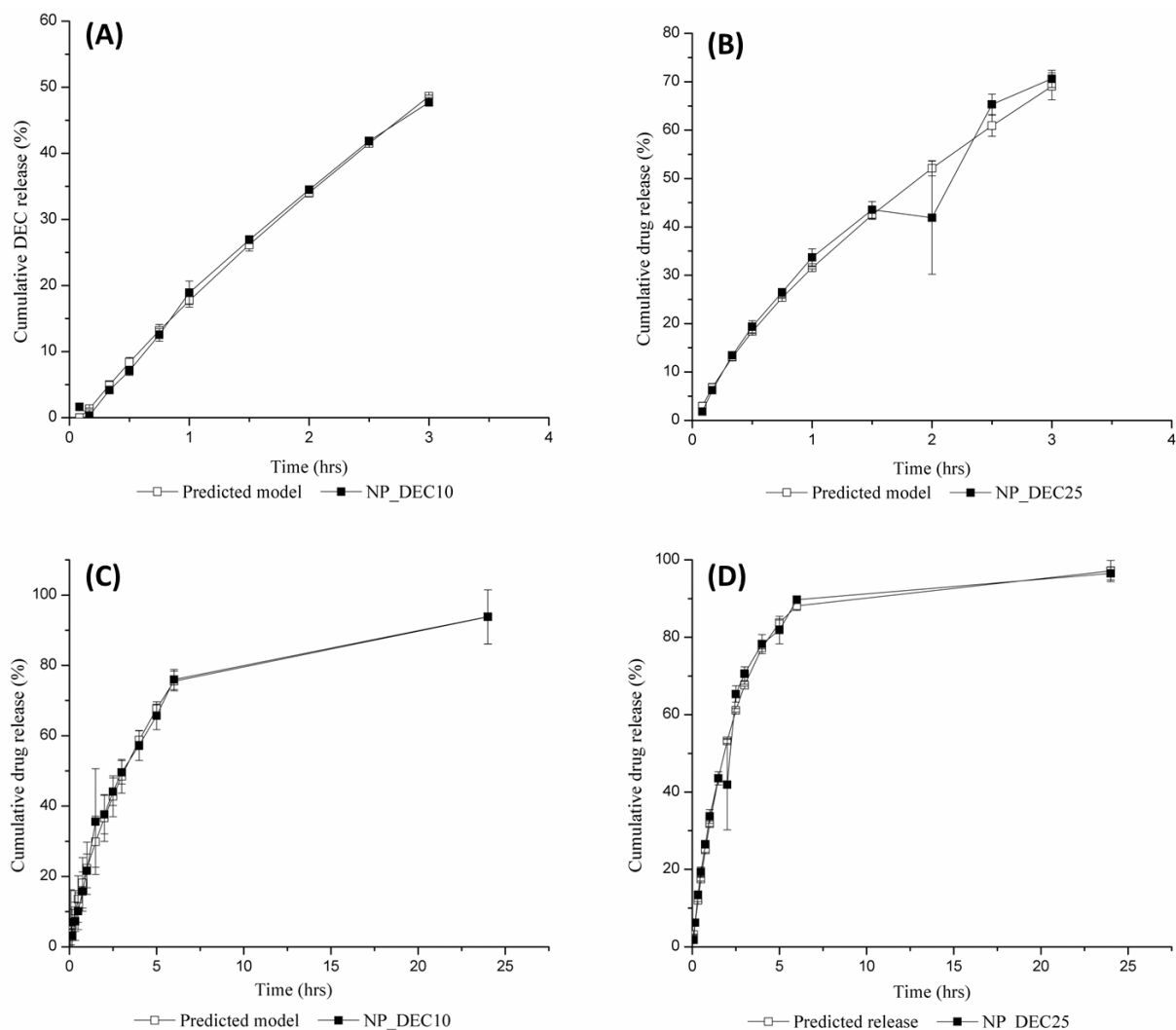


FIGURE 2 - *In vitro* drug release profile of (A) NP_DEC10 and (B) NP_DEC25 for 3 hours, and (C) NP_DEC10 and (D) NP_DEC25 for 24 h.

In vitro release data were fitted into mathematical equations; however, only the data from the initial 3h, or approximately 50% of drug release, were used (Figure 2) (Lafayette *et al.*, 1989). Most mathematical models fitted the data; however, the first-order kinetics, Korsmeyer-Peppas, and Peppas-Sahlin models demonstrated adjusted- $R^2 \geq 0.95$ and small RMSE. Furthermore, the Peppas-Sahlin model estimated that both formulations had their drug release driven by Fickian diffusion ($m = 0.29$). Thus, it is possible to conclude that drug release is concentration-dependent, as predicted by first-order kinetics (Lafayette *et al.*, 1989).

The cytotoxicity and biocompatibility evaluation of nanocarriers are crucial steps to ensure the safety

of nanomedicines. PCL products have been approved by health care authorities in several countries, and PCL nanoparticles are described as possessing high biocompatibility and low toxic effects (Kamaraj, *et al.*, 2017; Sinha *et al.*, 2004). Thus, our study further corroborates these reports, since no cytotoxicity was observed for DEC, blank nanoparticles, and DEC-loaded nanoparticles against the HUVEC line in a 24-hour assay (Figure 3). Additionally, the cell viability measured after 72 h demonstrated no decrease in DEC, NP_blank, and NP_DEC25 samples. In contrast, when NP_DEC10 was analyzed, an impact on cell viability was detected ($p\text{-value} \leq 0.05$). However, the concentrations evaluated were less than the tissue concentrations needed

for biological activity, as projected in our previous works. Therefore, this reduced cell viability may not have a major impact on their biological responses (Rodrigues *et al.*, 2018, 2017; Xin *et al.*, 2010).

Thus, the results of this study endorse the previous proposals to use a broader range of *in vivo* characterization for DEC-nanoparticles as they demonstrate good physical and physicochemical properties.

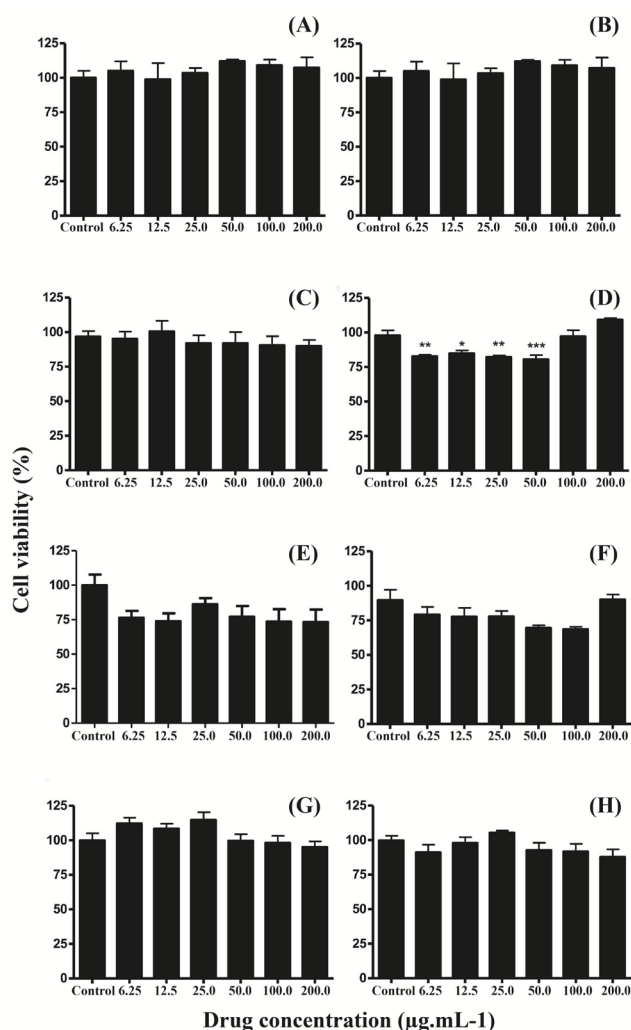


FIGURE 3 - Evaluation of the cytotoxicity at 24 h for (A) blank nanoparticles, (C) NP_DEC10, (e) NP_DEC25, (G) pure DEC; and at 72 h for (B) blank nanoparticles, (D) NP_DEC10, (F) NP_DEC25 and (H) pure DEC. *p<0,05; **p<0,01; ***p<0,001; ****p<0,0001 compared to the control group.

ACKNOWLEDGMENT

The authors are grateful for the financial support received from PROPESq/UEPB.

REFERENCES

Aguirre TAS, Teijeiro-Osorio D, Rosa M, Coulter IS, Alonso MJ, Brayden DJ. Current status of selected oral peptide technologies in advanced preclinical development and in clinical trials. *Adv Drug Deliv Rev.* 2016(Part B);106(3):223-41. doi:10.1016/j.addr.2016.02.004.

Ali M, Afzal M, Kaushik U, Bhattacharya SM, Ahmad FJ, Dinda AK. Perceptive solutions to anti-filarial chemotherapy of lymphatic filariasis from the plethora of nanomedical sciences. *J Drug Target.* 2014;22(1):1-13. doi:10.3109/1061186X.2013.832766.

Araujo TM, Teixeira Z, Barbosa-Sampaio HC, Rezende LF, Boschero AC, Duran N, Hoehr NF. Insulin-loaded poly(epsilon-caprolactone) nanoparticles: efficient, sustained and safe insulin delivery system. *J Biomed Nanotechnol.* 2013;9(6):1098-106.

Barba AA, Dalmoro A, D'Amore M, Vascello C, Lamberti G. Biocompatible nano-micro-particles by solvent evaporation from multiple emulsions technique. *J Mater Sci.* 2014;49(14):5160-70. doi:10.1007/s10853-014-8224-1.

Chaves LL, Rolim LA, Gonçalves MLCM, Vieira ACC, Alves LDS, Soares MFR, et al. Study of stability and drug-excipient compatibility of diethylcarbamazine citrate. *J Therm Anal Calorim.* 2013;111(3):2179-86. doi:10.1007/s10973-012-2775-7.

Ciardelli G, Chiono V, Vozzi G, Pracella M, Ahluwalia A, Barbani N, et al. Blends of poly-(epsilon-caprolactone) and polysaccharides in tissue engineering applications. *Biomacromolecules.* 2005;6(4):1961-76. doi:10.1021/bm0500805.

Costa A, Sarmento B, Seabra V. An evaluation of the latest *in vitro* tools for drug metabolism studies. *Expert Opin Drug Metab Toxicol.* 2014;10(1):103-19. doi:10.1517/17425255.2014.857402.

Fathima N, Mamatha T, Qureshi HK, Anitha N, Rao J V. Drug-excipient interaction and its importance in dosage form development. *J Appl Pharm Sci.* 2011;1(6):66-71.

Gressl C, Brunsteiner M, Davis A, Landis M, Pencheva K, Scrivens G, et al. Drug-excipient interactions in the solid state: the role of different stress factors. *Mol Pharm.* 2017;14(12):4560-71. doi:10.1021/acs.molpharmaceut.7b00677.

- Iqbal M, Valour JP, Fessi H, Elaissari A. Preparation of biodegradable PCL particles via double emulsion evaporation method using ultrasound technique. *Colloid Polym Sci.* 2015;293(3):861-73. doi:10.1007/s00396-014-3464-9.
- Kamaraj N, Rajaguru PY, Issac P kumar, Sundaresan S. Fabrication, characterization, in vitro drug release and glucose uptake activity of 14-deoxy, 11, 12-didehydroandrographolide loaded polycaprolactone nanoparticles. *Asian J Pharm Sci.* 2017;12(4):353-62. doi:http://dx.doi.org/10.1016/j.ajps.2017.02.003.
- Lafayette W, N.A. Peppas, J.J. Sahlin, Peppas NA, Sahlin JJ, N.A. Peppas, et al. A simple equation for the description of solute release. III. Coupling of diffusion and relaxation. *Int J Pharm.* 1989;57(2):169-72. doi:http://dx.doi.org/10.1016/0378-5173(89)90306-2.
- Mensink MA, Frijlink HW, van der Voort Maarschalk K, Hinrichs WLJ. How sugars protect proteins in the solid state and during drying (review): Mechanisms of stabilization in relation to stress conditions. *Eur J Pharm Biopharm.* 2017;114:288-95. doi:10.1016/j.ejpb.2017.01.024.
- Peixoto CA, Silva BS. Anti-inflammatory effects of diethylcarbamazine: A review. *Eur J Pharmacol.* 2014;734(1):35-41. doi:10.1016/j.ejphar.2014.03.046.
- Rodrigues GB, Oliveira EE, Junior FJBM, Santos LAM, Oliveira WH, França MER, et al. Characterization and evaluation of nanoencapsulated diethylcarbamazine in model of acute hepatic inflammation. *Int Immunopharmacol.* 2017;50(May):330-7. doi:10.1016/j.intimp.2017.07.014.
- Rodrigues GB, Oliveira EE, Junior FJBM, Santos LAM, Oliveira WH, França MER, et al. A new diethylcarbamazine formulation (NANO-DEC) as a therapeutic tool for hepatic fibrosis. *Int Immunopharmacol.* 2018;64(August):280-8. doi:10.1016/j.intimp.2018.09.010.
- Rocha SWS, Silva BS, Gomes FOS, Silva AKS, Raposo C, Barbosa KPS, et al. Effect of diethylcarbamazine on chronic hepatic inflammation induced by alcohol in C57BL/6 mice. *Eur J Pharmacol.* 2012;689(1-3):194-203. doi:10.1016/j.ejphar.2012.05.044.
- Silva BS, Rodrigues GB, Rocha SWS, Ribeiro EL, Gomes FOS, Silva AKS, et al. Inhibition of NF- κ B activation by diethylcarbamazine prevents alcohol-induced liver injury in C57BL/6 mice. *Tissue Cell.* 2014;46(5):363-71. doi:10.1016/j.tice.2014.06.008.
- Sinha VR, Bansal K, Kaushik R, Kumria R, Trehan A. Poly- ϵ -caprolactone microspheres and nanospheres: An overview. *Int J Pharm.* 2004;278(1):1-23.
- Xin H, Chen L, Gu J, Ren X, wei Z, Luo J, et al. Enhanced anti-glioblastoma efficacy by PTX-loaded PEGylated poly(ϵ -caprolactone) nanoparticles: In vitro and in vivo evaluation. *Int J Pharm.* 2010;402(1-2):238-47. doi:10.1016/j.ijpharm.2010.10.005.
- Zhang Y, Huo M, Zhou J, Zou A, Li W, Yao C, et al. DDSolver: An add-in program for modeling and comparison of drug dissolution profiles. *AAPS J.* 2010;12(3):263-71. doi:10.1208/s12248-010-9185-1.

Received for publication on 21st January 2019Accepted for publication on 07th February 2020